LORIENT CAMPAIGN 1993
The Dutch contribution

R.B. Boekema
TNO Physics and Electronics Laboratory
P.O. Box 96864
2509 JG The Hague
The Netherlands

SUMMARY

The performance of radar and infrared systems in a maritime environment is strongly dependent on the conditions of the atmosphere and the sea surface. In the autumn of 1993 an experiment was set up by the NATO Research Study Group AC/243 Panel3/RSG21 to collect propagation data at a line-of-sight propagation path. Purpose of the experiment was to gain knowledge about the behaviour of the path loss and angle of arrival of the signals.

This paper presents the results of the Dutch contribution to the experiment and a comparison of the measurements with model predictions. For radar in the line-of-sight situation the propagation is dominated by the multipath interference and influenced by ducting. Predictions performed with the propagation model PCPEMC [1] and the Bulk-CELAR [2] duct model show satisfying results for the position of the nulls, if wind speed and wave height are taken into account.

Using the data of this experiment, a synergism between radar and IR angle of arrival could not be proven.

1 INTRODUCTION

The performance of radar and infrared systems in a maritime environment is strongly dependent on the conditions of the atmosphere and the sea surface. The NATO Research Study Group AC/243 Panel3/RSG21 has conducted a measurement campaign near Lorient, France in the autumn of 1993. Purpose of this measurement campaign was to gain knowledge about the microwave and infrared propagation low above the sea at a line-of-sight propagation path. This is of great importance for the defence of ships against attacks by sea-skimming missiles. Special attention was paid to the behaviour of the angle of arrival for radar and infrared (IR) signals under the influence of ducting. The measurements at the radar frequencies are used to validate propagation model predictions.

This paper is based on the propagation data measured by the Dutch equipment and the meteorological data measured by a buoy halfway the propagation path. The microwave equipment consisted of an interferometer system at 16 GHz and an antenna array system at 10.5 GHz. The IR measurements were recorded with a line scanner in the 3-5 and 8-12 μm infrared bands.

For radar applications several models are available to predict the propagation under the influence of evaporation ducting. The PCPEMC model, based on the parabolic equation method is able to calculate the phase and amplitude components of the electromagnetic wave propagation. Input to this model is the duct height calculated by a bulk measurement model from the meteorological data measurements at the propagation path. These models and the expected propagation behaviour of the radar signals over the propagation path are presented in section 2.

The experiment is described in section 3. There, the microwave and the IR equipment are explained briefly. Also the location at the Atlantic ocean coast with the specific meteorological conditions encountered during the experiment is described.

The experimental results are given in section 4. This includes a comparison between microwave measurements and performed model predictions. The IR angle of arrival measurement results are also studied in this section.

In section 5 some conclusions are drawn about the angle of arrival behaviour for both radar and IR.

2 RADAR PROPAGATION

2.1 Theory

At the line-of-sight measurement configuration used, the propagation conditions are mainly determined by multipath. At the receiver location, the phase difference between direct waves from the transmitter and waves reflected at the sea surface creates a regular vertical lobing pattern of the electromagnetic field. If the direct and reflected waves have about the same phase, the values add up; if the direct and reflected waves have opposite phases, this results in cancellation of the electromagnetic fields. As a consequence, high path losses at certain altitudes occur. The locations of these high path losses are called interference nulls.

This field pattern caused by multipath is altered by a change in the structure of the atmosphere. Above sea the propagation is nearly permanently determined by the presence of an evaporation duct. This is a trapping layer caused by the characteristic refractivity profile in the lower atmosphere due to the evaporation of the sea water. The evaporation duct is characterised by its duct height. Under influence of the evaporation duct, the entire lobing pattern is bent downwards. This means that the height of an interference null decreases with increasing duct height.

For the used land-based measurement system also the tide has influence on the propagation between transmitter and receiver because their effective heights above the sea level change. From the point of view of the receiver, the interference pattern is lifted with increasing tide level.

Paper presented at the Sensor and Propagation Panel Symposium on "Propagation Assessment in Coastal Environments" held in Bremerhaven, Germany 19-22 September 1994.

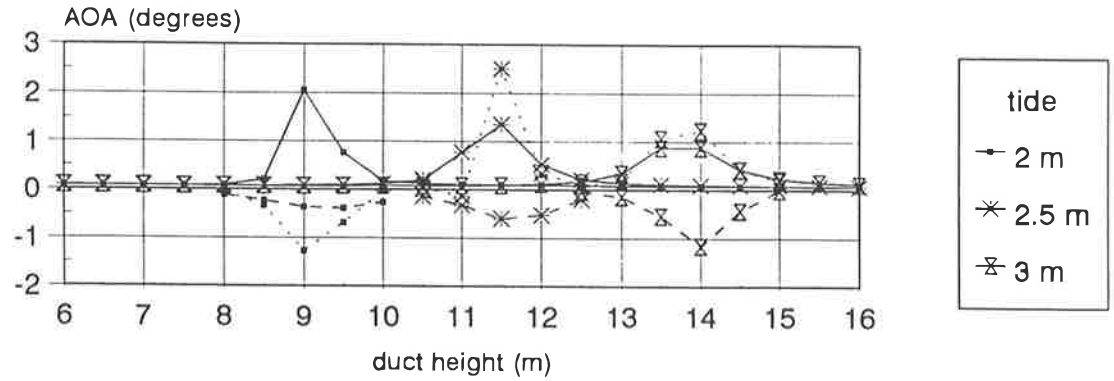

Fig. 1 PCPEMC angle of arrival predictions for Ku-band situation.

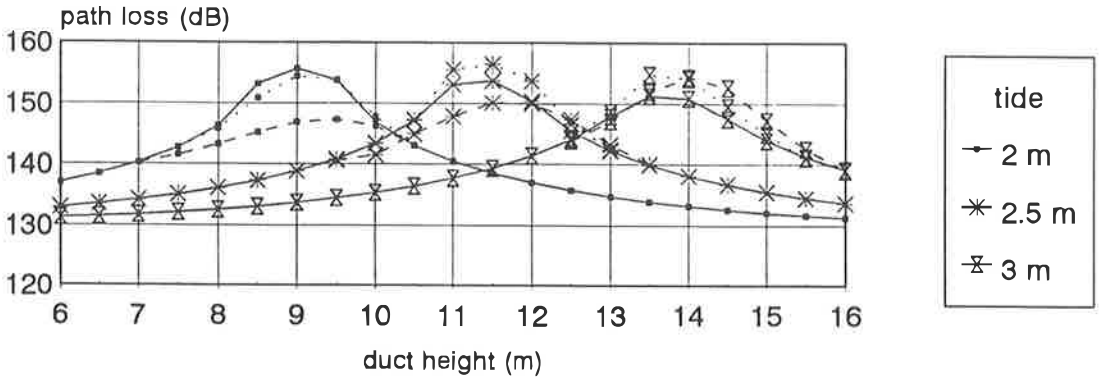

Fig. 2 PCPEMC path loss predictions for Ku-band situation.

2.2 Modelling

The modelling of the propagation is performed in two steps, as depicted in the next scheme.

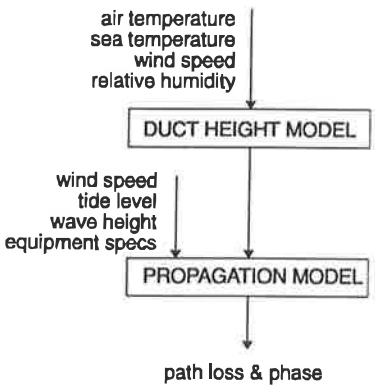

First the duct height model determines the refraction profile of the lower atmosphere based on the temperature of the sea and the parameters describing the condition of the air at one altitude ("bulk" measurement) above the sea level. This results in a duct height value. There are a number of models calculating the duct height using the "bulk" measurement method. They are all based on the Monin-Obukhof [3] boundary layer theory. In an unstable atmosphere (air temperature lower than sea temperature) they all give similar results.

The second step of the modelling, the theoretical predictions of path loss and angle of arrival is performed with a propagation model. There are a number of propagation models available as described in [4]. For the Lorient experiment the PCPEMC propagation model is used. This model based on the parabolic equation calculation is a version of PCPEM, adapted to produce the phase information apart from the path loss information. Input to the model are the variable values of duct height, the wind speed, the tide level, the wave height and the equipment specifications.

The tide level and wave height are used as a correction on the transmitter and receiver height.

The figures 1 and 2 show some results of the angle of arrival and path loss calculated for the Ku-band situation using the PCPEMC predictions. For three tide levels at the used measurement configuration the predictions are calculated over a duct height range from 6 to 16 metres. In the figures three wind speed situations are marked by the different line types. The solid line for a 5 m/s wind speed, the dotted line for 7.5 m/s and the dashed line for 10 m/s.

Extreme values of the angle of arrival only occur when the receiver is in an interference null, which can be correlated with the high path loss value. In all three tide cases this is the same null which occurs at the receiver at a different duct height, according to the tide and duct height theory in 2.1. In a null the direction and magnitude of the angle of arrival is strongly dependent on the wind speed. The wind speed influences the reflection coefficient at the sea surface. If the receiver is not in a null the angle of arrival is slightly positive (which means propagation slightly downwards) and nearly constant in value. At the 6 to 16 metre duct height range a small decrease in angle of about .02 degree was observed.
In the path loss figure one can see that the wind speed changes the depth of the nulls.

3 DESCRIPTION OF THE EXPERIMENT

The experiment is performed to investigate situations for the defence of warships against attacks by sea-skimming

missiles at a line-of-sight distance. For this purpose the location near Lorient was ideal with an island at about 10 kilometres from a peninsula at the Atlantic ocean coast.

The measurements have been performed at 10.5 GHz and 16 GHz.
The equipment consisted of separate transmitter and receiver combinations instead of radars. This has the advantage of a large cost reduction and a more reliable non-stop performance.

Both transmitters, consisting of a continuous wave (CW) source and a large parabolic reflector antenna mounted on a steady frame, were located on the island Ile the Croix, at a height of about 15 metre above average sea level.

The receivers were positioned at the beach of the peninsula of Gâvres separated from the transmitters by 9.7 kilometres of open sea. They were mounted on top of a cabin containing the registration equipment at a height of about 10 metres above average sea level. Both receivers, specially build to derive power and phase information from the received signal, worked with different techniques.

The 16 GHz interferometer consisted of a 2 element vertical array. The array elements were pyramidal horns with a 24 cm aperture connected to the receiver with a 90° hybrid component. From the output signals of the hybrid the amplitude and phase information of the signals received by the two antennas can be derived.
The output signals of the hybrid were registered by a computer with an AD-converter, and processed afterwards.

The 10.5 GHz signal was received by a vertical array of 10 horizontally polarised microstrip antenna elements. The centre 8 elements were used for the actual signal measurements. The receiver is coherent, with the phases of the received signals of each of the eight elements determined with respect to the phase of the top element. The eight antenna elements can be sequentially linked with a common receiver channel through a multiplex PIN diode switch. A measurement scan of the eight antenna elements is executed in 1 millisecond, fast enough to consider it as an instantaneous measurement. The eight antenna signals are processed and stored in memory in a 12 bits I and Q format.

The angle of arrival (AOA) is calculated from the phase data by

$$\mathrm{AOA}=\mathrm{ARCSIN}\ \frac{d\Phi\,\lambda}{2\,\pi\,D}\ ,$$

in which $d\Phi$ is the phase difference between the antenna signals, D the distance between the antennas and λ the wavelength of the received signal. The maximum unambiguous angle of arrival range for the 16 GHz interferometer is ± 2.4° and for 10.5 GHz ± 7.2° if the antenna is configured as two arrays of four adjacent antennas.

The radar propagation measurements at both frequencies are performed every 5 minutes. To eliminate small disturbing effects like those from small waves, every measurement consist of a sequence of samples.
At 16 GHz eight samples of the two channels are taken with an interval of 10 μseconds to get one record. Ten of these are taken at an 1 second interval. This data is averaged to get one measurement.
At 10.5 GHz sixteen scans of the eight antennas are taken directly after each other to get one record in 16 mseconds. Ten of these records, taken with an 1 second interval are averaged.

IR measurements were performed simultaneously with the radar measurements over the same 9.7 kilometre path. The measurements were recorded with the TNO-FEL WBS-3 line scanner in the 3-5 and 8-12 μm infrared bands. This instrument was positioned next to the receivers on the mainland. The IR sources were placed at two heights on the island, one next to the radar transmitters at about 15 metres and one higher on the cliff at about 38 metres above average sea level. The positional accuracy of the instrument was 0.35 mrad. IR-measurements were performed only over short periods of the day for several reasons: the line scanner needs regular maintenance during measurements, it cannot operate during rain and the data processing has to be performed manually.

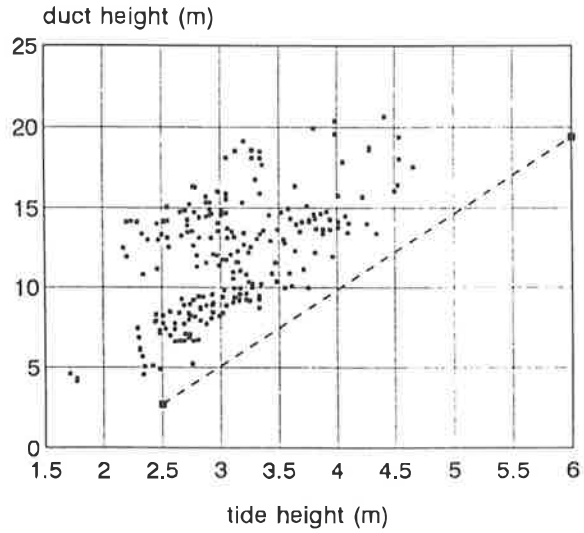

Fig.3 Occurrence of the nulls at X-band with Paulus duct height and no tide correction.

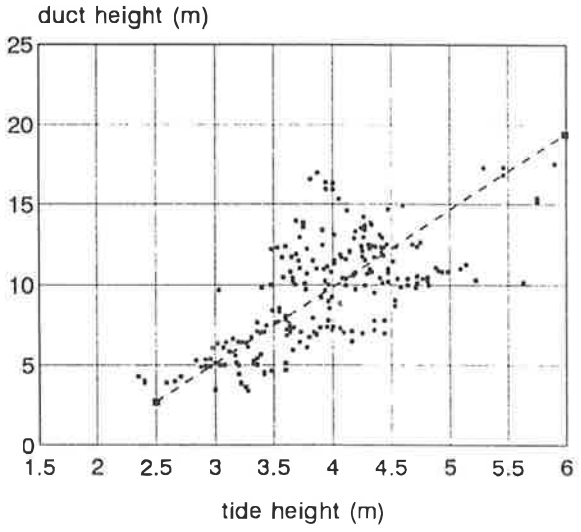

Fig.4 Occurrence of the nulls at X-band with Bulk-CELAR duct height and wave height correction on tide.

Halfway the propagation path, two French buoys were anchored: a waverider buoy to measure the wave spectrum of the sea, and a meteorological buoy to collect the data necessary for the duct modelling. The meteorological buoy recorded the air and sea temperature, wind speed, air humidity, and also the solar flux and wind direction as supplementary information.
At this part of the Atlantic Ocean the tidal variation is large. It can reach values of up to 5 meters. This information is registered at a local weather station at the coast.

4 EXPERIMENTAL RESULTS

The weather conditions during the experiment were rough for the time of the year. There were periods with storms and the amount of rainfall was twice the normal amount at the end of September and even three times the normal amount for October. The conditions along the path were representative for open sea conditions because the wind direction was mainly from the sea. Therefore the atmosphere was most of the time unstable, indicating an air temperature lower than the sea temperature, and securing a reliable prediction of the duct height. More than 90 percent of the duct heights were between 6 and 16 meters.

A way to validate the model predictions with the measurements is to consider the nulls. As indicated by the figure 1 and 2, the nulls are characterised by high path loss values and an extreme angle of arrival behaviour. For these predictions it appears that, when there is a null at the receiver for specific duct and tide combinations, the duct heights and tides seem to have a nearly linear relation.

Figures 3 and 4 show the relation between the measurements and predictions for the nulls at X-band. For these figures, situations with high path losses and extreme angles of arrival have been selected from the measurement data. The duct and tide heights at these conditions are presented by points in the figure. The line in the figure indicates the PCPEMC prediction.
In figure 3 the actual tide height and the duct height calculated with the Paulus formulation [5] is presented. The correlation with the model prediction in the figure is very poor, in all cases the Paulus duct height is at least four metre to high. This corresponds with the experiences at former propagation experiments on over-the-horizon paths [6].

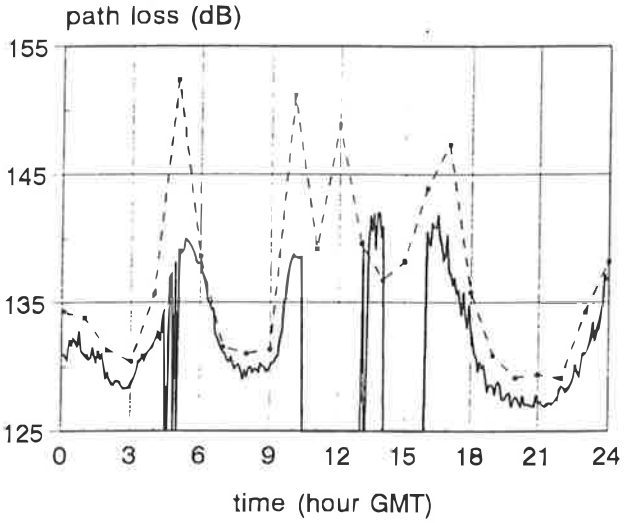

Fig.5 X-band path loss of 28 September.

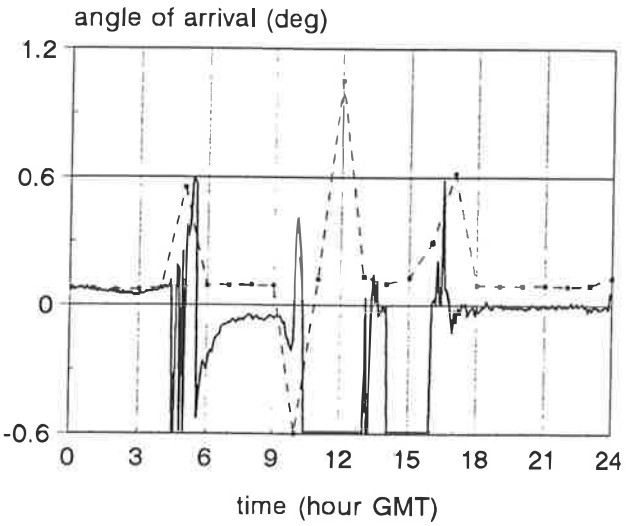

Fig.6 X-band angle of arrival of 28 September.

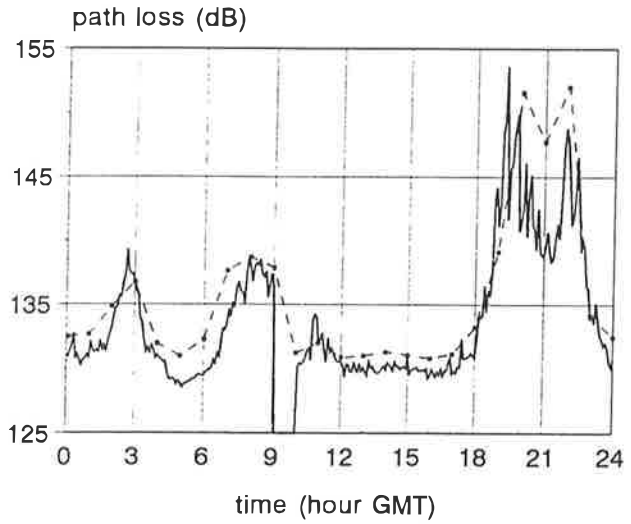

Fig.7 Ku-band path loss of 28 September.

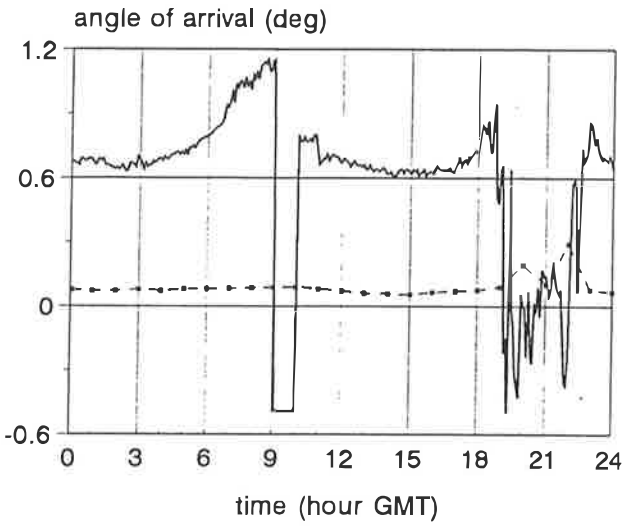

Fig.8 Ku-band angle of arrival of 28 September.

In figure 4 the duct height calculated with the Bulk-CELAR model is used, this results in smaller duct heights. The tide height in this figure is corrected with the H1/3 (significant) wave height value measured by the waverider buoy. This shifts the points measured under rough sea conditions to the right.
The correlation between these measurements and the predictions is good.

To get a good impression of the overall model performance, the results of the model must be compared with the path loss and angle of arrival for a wide variety of tides and meteorological situations. In this section the results of one representative day are presented in detail. The PCPEMC predictions at X and Ku band of 28 September 1993 are calculated for every hour and compared with the measurement data. Although only one day is presented, the conclusions are based on the general behaviour, encountered during the entire measurement campaign.

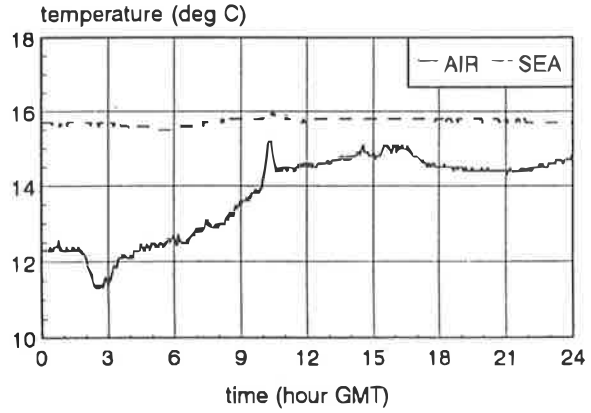

Fig.9 Air and sea temperature at 28 September.

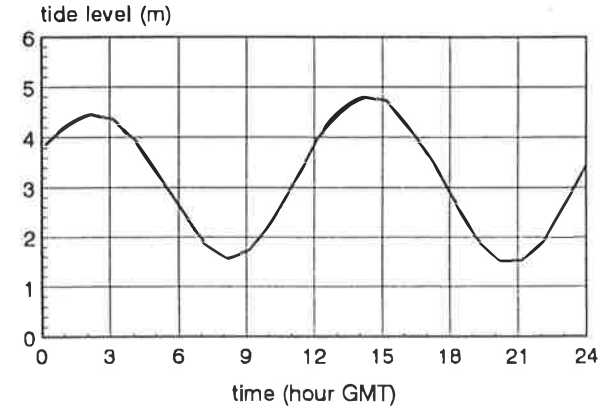

Fig.10 Tide variation at 28 September.

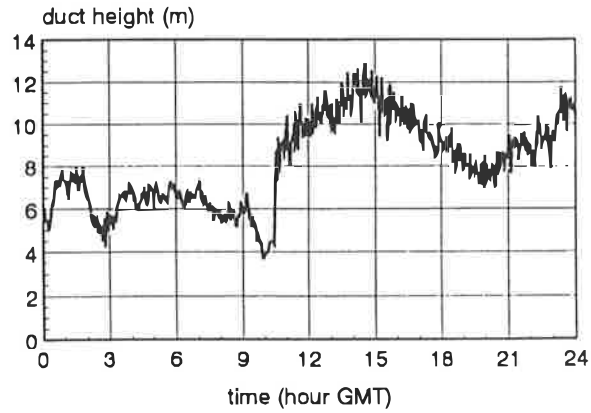

Fig.11 Bulk-CELAR duct height at 28 September.

4.1 X-band sample day

Figures 5 and 6 present the path loss and angle of arrival (AOA) at X-band. The measurements are presented by the solid line, and the PCPEMC predictions by the points connected by the dotted line. Unfortunately there is some loss of measurement data due to calibration and back-up activities, like around 12:00 and 15:00 hour, and due to locking problems like at 5:00 hour. The PCPEMC predictions are performed with the Bulk-CELAR duct height and with the sea level corrected with the H1/3 wave height.
Comparing the measured and predicted path loss one observes that they agree well, though the predicted path loss is generally a few dB higher than the measured one. The measured nulls are predicted at the right time, but they are not as deep (high path loss value) as predicted.

Looking at the measured and predicted AOA, one also observes a prediction of the nulls (high angles of arrival) at the right time.
For the measurement configuration used, an error occurs at low tide situations because the individual antenna elements have picked up reflections from the beach. This effect is minimised by configuring the eight antenna elements as two arrays of four antennas, thereby limiting their field of view, but it still results in a negative offset at low tide. This is visible between 7:00 and 9:00, and between 18:00 and 24:00 hour.

4.2 Ku-band sample day

Figures 7 and 8 present measured and PCPEMC predicted path loss and AOA at Ku-band. Due to back-up activities some measurement data is missing between 9:00 and 10:00 hour. The PCPEMC predictions, presented by the points connected with the dotted line, are also calculated with the Bulk-CELAR duct height and the sea level corrected with the H1/3 wave height.
Comparing the measured and predicted path loss one again observes that the predicted path loss is generally only a few dB higher than the measured one, apart from the times when nulls occur. The measured nulls are predicted at the right time, but they are not as deep (high path loss value) as predicted.
The measured and predicted AOA show a large difference. Although showing the same trends, the measured AOA is much larger than the predicted one. If not in the null, the deviation is about a factor ten, but in the null it is much smaller. The reason for this large AOA deviation is still unknown. It is probably a result of a wrong system calibration, but it will be point of further research.

Figures 9, 10 and 11 show some of the parameters used for the modelling at 28 September. Figure 9 presents the air and sea temperature, the tidal variation is presented in figure 10 and the calculated Bulk-CELAR duct height in figure 11.

If the X and Ku band figures are compared one sees very different shapes. For this day the nulls at the two frequencies manifest at different moments, but that is no general rule. With this measurement configuration the

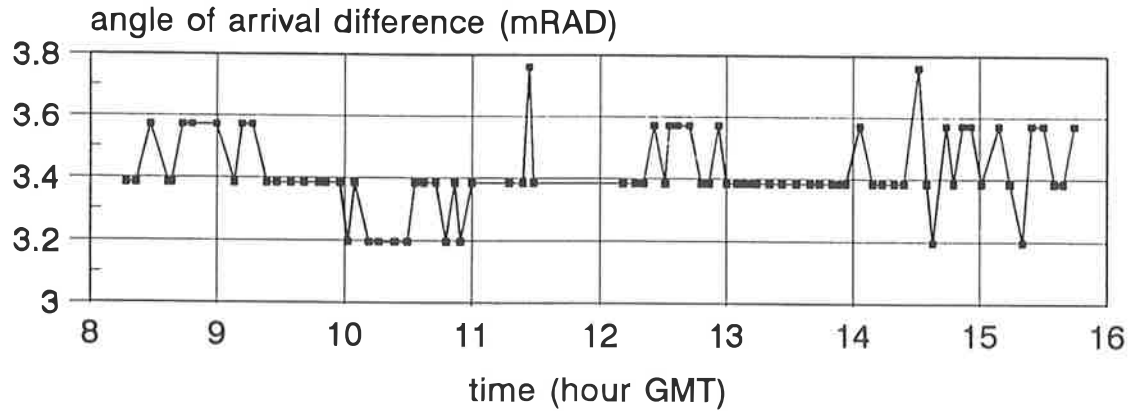

Fig.12 IR angle of arrival difference measured in the 4μ band at 28 September.

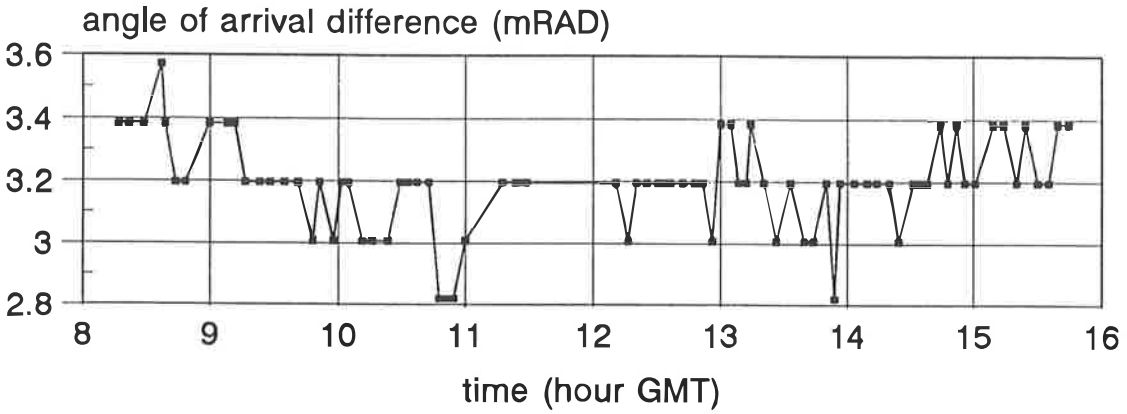

Fig.13 IR angle of arrival difference measured in the 10μ band at 28 September.

model predicts no simultaneous nulls at the two bands for the duct range from 6 to 16 meters, but this is dependent on the heights of the equipment above the sea level. In general we can conclude that the model performance concerning the prediction of the nulls is satisfying. In an operational situation, a radar performance prediction program can be used as a decision tool to select the radar frequency which gives optimum performance under the actual circumstances.

4.3 Infrared data

At the same day the IR data in the 4μ and 10μ bands has been measured between eight and sixteen hour. Although very small, the IR AOA variation at this day was more than on average. The figures 12 and 13 present the AOA difference between the two sources (ΔAOA). At both bands one can see a clear decrease in ΔAOA between eight and eleven, followed by a recovery and a small increase. Between eight and nine an IR subrefraction case is present. This correlates with the large negative air and sea temperature difference early in the day (fig.9).
A direct correlation with the CELAR duct height can not be found, and also not with the radar AOA. The total measured ΔAOA variation is .8 mRAD (0.046 deg).

5 CONCLUSIONS

At the X and Ku-band radar line-of-sight situation the propagation is dominated by the multipath interference and influenced by ducting.

The path loss shows a large variation due to the lobing structure of the interference pattern. The angle of arrival is slightly positive except for the short periods when the receiver is located in an interference null. The angle of arrival then increases very fast, to values of up to more than 2 degrees. Dependent on the wind speed this angle can be positive or negative.

Predictions have been performed using the propagation model PCPEMC and the Bulk-CELAR duct model.
These model predictions based on simple one spot meteorological measurements show satisfying results for the position of the nulls.
Important for the model predictions is the correction of the sea level with the wave height.
In general the measured path losses in the nulls are not as high as predicted. Accurate prediction of the angle of arrival in the null is not possible while the angle of arrival behaviour is very critical.

Angle of arrival measurements in the IR band are also influenced by the meteorological conditions, but show no extremities as in the radar band. The behaviour can not be correlated with the radar duct height. The small IR data set and the nearly constant stability of the atmosphere does not allow further comparison.

In an operational situation, a radar performance prediction program can be used to predict the occurrence of interference nulls in the actual environment. The occurrence of these nulls can then be remedied by either

switching to another radar frequency or by relying more heavily on the infrared equipment.

ACKNOWLEDGEMENTS

We would like to acknowledge our collegues from CELAR, CERT, DREV, FGAN and NCCOSC for their cooperation in this campaign.

REFERENCES

[1] Craig, K.H. and Levy, M., "PCPEM software program.", Signal Science Limited, Abingdon, Oxon, UK, 1990.

[2] Claverie, J., "Determination des profils meteorologiques dans le conduit d'evaporation", ASRE/16 437, CELAR, Bruz, France, 1990.

[3] Monin, A.S. and Obukhof, A.M., "Basic laws of turbulent mixing in the ground layer of the atmosphere", Akad. Nauk. USSR, Geofiz. Inst. Tr., 1954.

[4] Vogel, M.H., "A comparison between several computer codes for calculations on microwave propagation.", FEL-29-A435, FEL-TNO, The Hague, The Netherland, 1992.

[5] Paulus, R.A., "Specification for environmental measurements to assess radar sensors.", TD-1685, NCCOSC, San Diego, California, USA, 1989.

[6] Boekema, R.B., "Comparison of the results from the propagation experiments at the Atlantic Ocean and Mediterranean Sea coast.", FEL-93-B150, FEL-TNO, The Hague, The Netherlands, 1993.